water

MDPI

Article

The Downscaling Study for Typhoon-Induced Coastal Inundation

Dongmin Jang, Wonkyun Joo, Chang-Hoo Jeong, Wonsu Kim, Sung Won Park * and Yoojin Song

Department of Data-centric Problem-Solving Research, Korea Institute of Science and Technology Information (KISTI), Daehak-ro, Yuseong-gu, Daejeon 34141, Korea; jmin@kisti.re.kr (D.J.); joo@kisti.re.kr (W.J.); chjeong@kisti.re.kr (C.-H.J.); wonsukim@kisti.re.kr (W.K.); syj7@kisti.re.kr (Y.S)

* Correspondence: swpark@kisti.re.kr; Tel.: +82-42-869-1624

Received: 27 February 2020; Accepted: 10 April 2020; Published: 13 April 2020

Abstract: Typhoons can often cause inundation in lower coastal cities by inducing strong surges and waves. Being affected by typhoon annually, the coastal cities in South Korea are very vulnerable to typhoons. In 2016, a typhoon 'CHABA', with a maximum 10 min sustained wind speed of about 50 m/s and a minimum central pressure of 905 hPa, hit South Korea, suffering tremendous damage. In particular, 'CHABA'-induced coastal inundation resulted in serious damage to the coastal area of Busan where a lot of high-rise buildings and residential areas are concentrated, and was caused by the combined effect of tide, surge, and wave. The typhoon-induced surge raised sea levels during high tide, and the strong wave with a long period of more than 10 s eventually led to the coastal inundation at the same time. The present research focuses a numerical downscaling considering the effects of tide, surge and wave for coastal inundation induced by Typhoon 'CHABA'. This downscaling approach applied several numerical models, which are the Weather Research and Forecasting model (WRF) for typhoon simulation, the Finite Volume Community Ocean Model (FVCOM) for tide and surge simulation, and the Simulating WAve Nearshore (SWAN) for wave simulation. In a domain covering the Korean Peninsula, typhoon-induced surges and waves were simulated applying the results simulated by WRF as meteorological conditions. In the downscaled domain ranged near the coastal area of Busan, the coastal inundation was simulated blending a storm tide height and an irregular wave height obtained from the domain, in which each height has 1 s interval. The irregular wave height was calculated using the significant wave height and peak period. Through this downscaling study, the impact of storm tide and wave on coastal inundation was estimated.

Keywords: downscaling; surge; wave; coastal inundation; numerical modeling

1. Introduction

The increase of sea temperature due to climate change may cause the sea level to rise and an increase of typhoon intensity, leading to extreme damages from flood disaster in coastal areas, including river mouth and river reaches [1–10]. Coastal flooding can be driven by water level rise due to a combination of tide, surge, and wave, and it can be maximized by the breaking and run-up of strong waves during high sea level by high tide and storm-induced surge [11,12]. In addition, undesirable erosion and loss of beaches along the coastline have continuously been generated with extreme flood events and storm-induced surge [13–21]. An aerial photograph of the dunes located between the French and Belgian borders confirms that the speed of retreat in front of sand dunes has increased for 30 years [14]. The most severe Atlantic and Gulf Coast storms in the U.S. reveals the primary factors affecting morphological storm responses of beaches and barrier islands [15]. Dune

erosions and cross-shore beach profile evolution occurred in Outer Banks, North Carolina, in 2003 during Hurricane Isabel, were analyzed with several LIDAR (Light Detection And Ranging) profiles before and after Hurricane Isabel for two months [16]. It is a surveying method with laser light for measuring the reflected light with a sensor and commonly used to make high-resolution maps.

The need for scientific, accurate, fast, and efficient forecasting of extreme weather-induced disasters in coastal regions on sustainable socio-economic development plans has been increasing all over the world. There is no known way to prevent a coastal disaster in the short term, but if there is information about when it will happen and what kind effect it is likely to have, damage from the disaster could be minimized and costs of subsequent repairs reduced. In the decision-making process for response to flooding-induced disasters, it is important that information about the occurrence of disaster is accurate. Over the last decade, considerable researches have been focused for the accurate prediction of surge, wave and coastal inundation, it is possible to resolve the coastal geometry more precisely through unstructured grid model: advanced circulation model (ADCIRC), and finite-volume community ocean model (FVCOM) [2,22–31]. Also, in recent years, a fully coupled wave-current model with unstructured grid has been used to improve accuracy of surge prediction because the typhoon-induced surface wave plays important role in the surge and coastal inundation [1]. However, a lot of computing resource and cost is required for the fully-coupled modeling with high resolution of unstructured grid. Therefore, high-performance computing (HPC) is necessary in the field for finding useful information from large, complex, and rapidly growing volumes of data and analysis. Although several researches with model lightening were presented, HPC was needed in this research because more detailed simulation and analysis are needed [22,23]. Therefore, we used the HPC system of the Korea Institute of Science and Technology Information (KISTI), which is funded by the Korean government for the HPC service in South Korea.

In this study, we selected typhoon 'CHABA' (1618), which caused huge damage to South Korea in 2016, the case study, and simulated the typhoon, typhoon-induced storm surge, and inundation in Busan, the second largest, and a coastal city in South Korea. This paper presents our finding to answer the following: (1) How much affected by typhoon 'CHABA' was Busan city? (2) How accurately can we predict the actions of typhoon CHABA and typhoon-induced disasters?

2. Methodologies

2.1. Prediction and Analysis System

KISTI was designated the 'National Supercomputing Center' in 2011. Using HPC, we have been developing the prediction and analysis system to respond to natural disasters such as typhoons, storm surges, and other flooding. It is an integrated package system that collects various data based on scenarios and produces forecasting information, analyzes the likely socio-economic impacts, and visualizes the simulated results. Initial conditions established from the TMD (tide model driver) and HYCOM (hybrid coordinate ocean model) were applied in the surge and wave prediction. With calculated results of the irregular wave height from JONSWAP (Joint North Sea Wave Observation Project), surge and wave predictions were adopted in the flood inundation model (Figure 1).

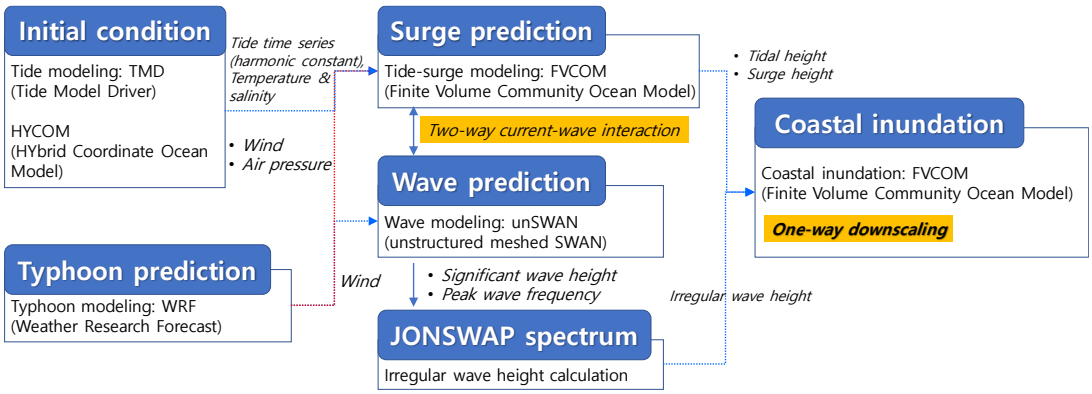

Figure 1. Conceptual diagram of analysis system and data processing.

2.2. A Case Study: Typhoon 'CHABA' (1618)

Typhoon 'CHABA', which was the 18th numbered storm, ranked third in intensity among the tropical cyclones in 2016, and was the most powerful typhoon to make landfall in South Korea since the typhoon 'SANBA' in 2012 [9]. The CHABA in early October 2016 was the third strongest typhoon after the typhoon 'MAEMI' in September 2003 and Typhoon 'Lussa' in August 2002, with a maximum wind speed of 56.7 m/s [10]. In 2016, many typhoons have passed in many Asian countries including South Korea and China. Representative strong typhoons include LionRock, Meranti, Melakas, and Megi, and their impact analysis has been studied [11].

It developed approximately 1445 km east-northeast of Guam on 26th September, moved westward, and started to move northward on 1st October. The typhoon intensified to a category 5-equivalent super typhoon on the Saffir-Simpson Hurricane Wind Scale (SSHWS) with its eye surrounded by a very intense convective core due to very warm sea surface temperatures. The peak of 1 min sustained wind and 10 min sustained wind was 75 m/s (270 km/h) and 50 m/s (180 km/h), respectively, and its lowest pressure was 905 hPa. The CHABA gradually weakened as its core became asymmetric, and dropped in strength to a strong Category 4 typhoon by 4 October. The storm caused massive damage to the southern coastal cities in South Korea, especially Busan, which is the second largest city in South Korea and has regions of dense population along the coastline. In South Korea, there was loss of life, with at least seven people killed and four people missing during that period. Hundreds of flights were cancelled and the electricity was off in more than 200,000 households. There was also flooding in the cities of Ulsan, Gyeongju, and Busan, with damage estimated at 20.3 billion KRW (18.3 million USD) according to the Korea Standard Times in 6th October 2016.

2.3. Numerical Model Description

We developed a high-resolution atmospheric, oceanic, and inundation (flooding) prediction and analysis system with the aim of producing more scientific, more accurate, faster, and more efficient forecasting of typhoon-induced disasters based on a HPC system. Using this integrated and coupled prediction system, the coastal inundation caused by the typhoon was simulated (Figure 2). Tables 1, 2 and 3 show the description of the typhoon, surge and wave modeling using Weather Research and Forecasting model (WRF), the Finite Volume Community Ocean Model (FVCOM), and the Simulating WAve Nearshore (SWAN), respectively. WRF model is a numerical weather prediction (NWP) system designed to serve both atmospheric research and operational forecasting needs. The effort to develop WRF began in the 1990's and was a partnership with the National Center for Atmospheric Research (NCAR), the National Oceanic and Atmospheric Administration (NOAA), the U.S. Air Force, the Naval Research Laboratory, the University of Oklahoma, and the Federal Aviation Administration (FAA) in the United States. NWP refers to the simulation and prediction of the atmosphere with a computer model, and WRF is a set of software for this. The FVCOM model is an unstructured-grid, free-surface, three-dimensional equation coastal ocean model. This model is developed by researchers at the University of Massachusetts Dartmouth and Woods Hole Oceanographic Institution. Obviously, developed for the estuarine flooding and drying process, it has been upgraded to the spherical coordinate system of basin and global applications. Lastly, SWAN computations can be made on a regular, a curvilinear grid, and a triangular mesh in a Cartesian or spherical coordinate system. It is developed at Delft University of Technology, that computes random, short-crested wind-generated waves in coastal and inland regions.

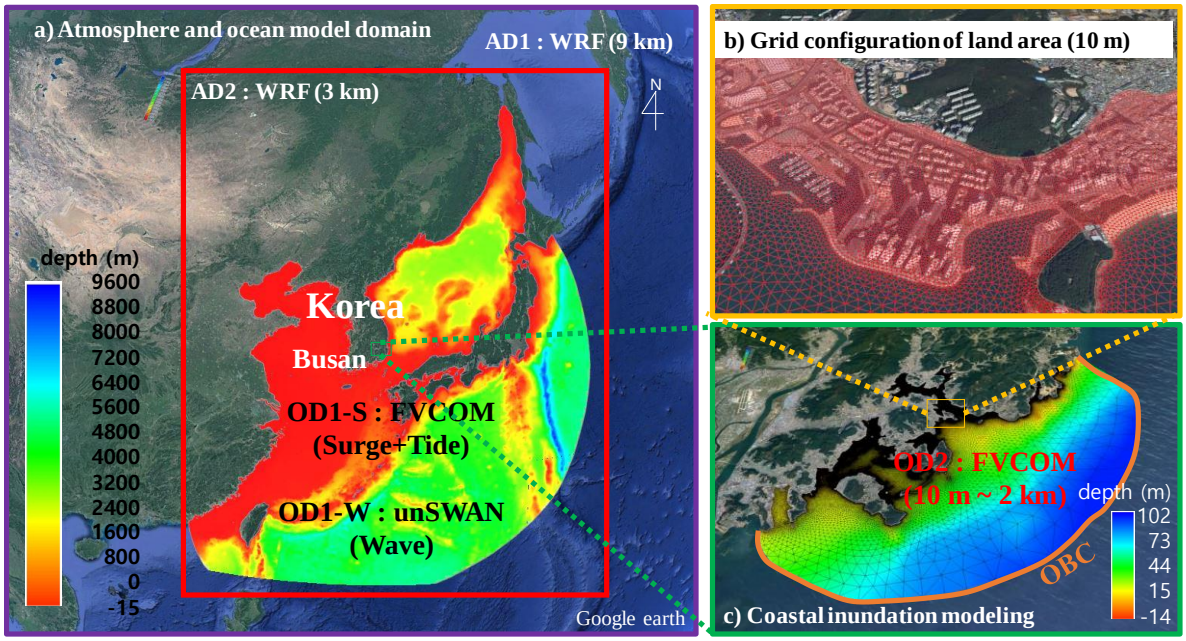

Figure 2. Model description for simulation of typhoon-induced coastal inundation (AD: Atmosphere Domain, OD: Ocean Domain).

Table 1. Model description of the typhoon.

Items		AD1	AD2
Model		WRF 3.7.1	
Initial and boundary		NCEP/FNL (0.25-degree)	
Horizontal resolution		9 km	3 km
Vertical level		41	41
Numerical grid		600 × 600	1099 × 1321
Physical specs.	Microphysics	WDM6	
	Cumulus	Kain-Fritsch	-
	PBL	YSU PBL	
	Radiation	RRTMG(LW)	RRTMG(SW)
	Land surface	NOAH LSM	
● AD (Atmosphere Domain)			

Table 2. Model description of the surge.

Items	OD1-S (Surge Modeling)
Model	FVCOM 3.2.1
Atmospheric condition	AD2 of WRF modeling (3 km)
Open boundary	Tidal Model Driver (TMD)
Dimension	2D
Number of cells	602,807
Horizontal mixing	Smagorinsky's parameterization
● OD (Ocean Domain)	

Table 3. Model description of the wave.

Items	OD1-W (Wave Modeling)
Model	SWAN 40.85
Atmospheric condition	AD2 of WRF modeling (3 km)
Initial condition	36 wave direction (10° interval)

	31 wave direction (0.031–0.54 Hz.)
Number of cells	602,807
Breaking index	γ = 0.73
Bottom friction	JONSWAP formulation (C_b = 0.067 m^2s^{-3})

For the CHABA hind-cast (from 3rd to 6th in October; 72 h), high resolution WRF was applied using reanalysis data produced by NCEP/FNL (National Center for Environmental Prediction/Final) 0.25-degree for the boundary and initial conditions. The horizontal resolution of two domains (AD1 and AD2) in WRF simulation, considering two-way nesting, was 9 km (600 × 600) and 3 km (1099 × 1321), respectively (Figure 2), and the number of vertical layers was 41. High-resolution data (wind speed, direction, and pressure) in AD2 were used as the meteorological input of surge and wave simulation.

For the simulation of the typhoon-induced coastal inundation, the 1-way downscaling technique was applied using an unstructured grid model, FVCOM for surge and SWAN (simulating wave nearshore) for waves. The grid generation of FVCOM and SWAN in OD1 is exactly the same, and the number of unstructured grids with variable resolution ranging from 10 m to 2 km was 602,807.

First, the wind and pressure of AD2 produced by WRF was used as the initial and boundary condition to simulate the surge (FVCOM) and wave (SWAN) in a mother domain in ocean modeling. Then, the coastal inundation in the downscaled domain (OD2) ranged near Busan was predicted using FVCOM (Figure 2). To consider the effects of both surge and waves, the surge and waves data obtained from the mother domain (OD1-S and OD1-W) was combined and applied in the simulation. The number of unstructured grids in the downscaled domain (OD2) used to simulate the coastal inundation, was 315,909 and the minimum resolution was approximately 10 m.

To account for the effect of wave on the coastal flooding, we first generated an irregular waves height using JONSWAP spectrum [32] based on the wave model (OD1-W) results (significant wave height and peak frequency). JONSWAP spectrum is the following as:

$$S_j(\omega) = \frac{\alpha g^2}{\omega^2} \exp\left[-\frac{5}{4}\left(\frac{\omega_p}{\omega}\right)^4\right]\gamma^r \quad (1)$$

$$r = \exp\left[-\frac{(\omega-\omega_p)^2}{2\sigma^2{\omega_p}^2}\right] \quad (2)$$

where H_s, w_p, α, γ and σ are the significant wave height, peak frequency, the slope parameter, peak enhancement factor and relative measure of the width of peak (0.07 or 0.09), respectively. In this research, we assumed that α is 0.0081 and γ is 1.6. The number open boundary nodes in the OD2 model is 45, and the irregular wave height was generated and applied at each open boundary. Figure 3 shows the irregular wave height using JONSWAP spectrum at the 1st node of open boundary in OD2.

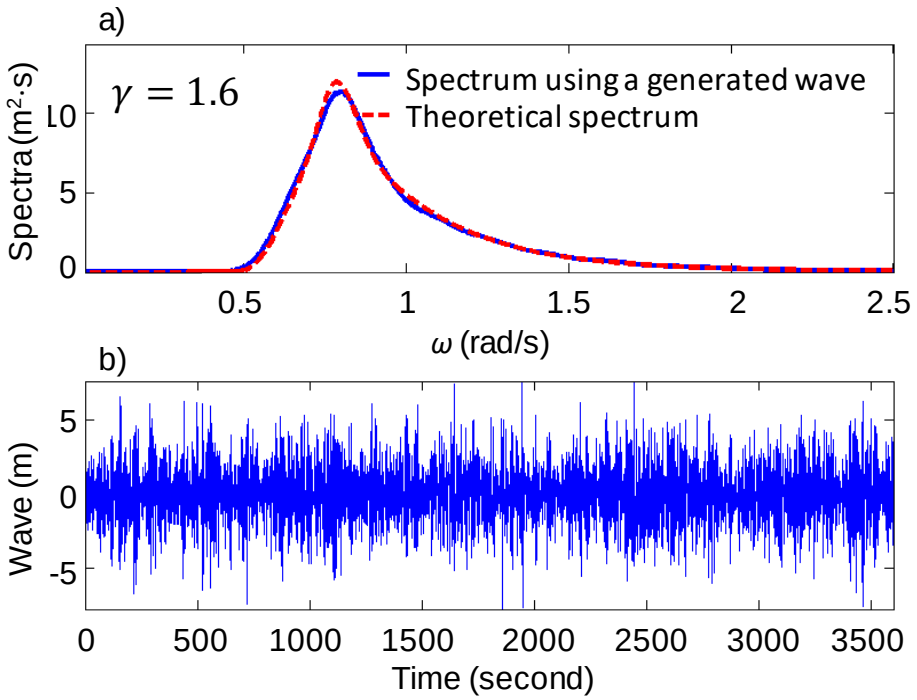

Figure 3. Comparison of the irregular wave height: (**a**) comparison between generated wave spectrum and theoretical spectrum, (**b**) irregular wave height (m) at the node located in the middle of the open boundary line.

As we compared the spectrum of generated irregular wave with theoretical spectrum, two spectrums are almost identical. The generated wave time signal from spectrum with 1 s interval was combined with surge height with 1 s interval, and we observed that the seawater flooding occurs near the lower coastal region. The computation time for typhoon modeling, surge and wave modeling, and inundation modeling was about six hours, 30 min and one hour, respectively using about 50 TF (terra Flops per second) of KISTI's Tachyon 2 system (SUN Blade 6275, Rpeak is about 300 TF). Also, the size of each data set of three models was (400, 200, and 100) GB, respectively. Relatively large computing resources are required for typhoon modeling in the prediction system. For faster and more efficient typhoon prediction, it might be necessary to develop a parallel computing technology for use in the GPU (Nvidia's Graphic Processing Unit) or KNL (Intel's KNights Landing) environment.

3. Results and Discussion

The downscaling technique was applied to improve numerical model accuracy owing to the limitation of computational resources in this research. To compare the regional variation, major stations were selected near the shoreline in south coast of the Korean Peninsula including Jeju island (Figure 4). The meteorological forcing plays dominant role in surge and wave, and the error of meteorological forcing results in problem of the timing of peak surge and wave in the modeling. If the accuracy of the atmospheric model is secured, the accuracy of the surge and wave simulation can be also secured. First of all, the simulated data of typhoon modeling using WRF was compared with the observation data (wind speed, direction, and pressure) at five locations near shore (Figure 5). When the typhoon 'CHABA' reached near South Korea, maximum wind speed is about 30 m/s, and minimum pressure is about 960 hPa. The simulated results of wind speed and direction are similar with observation data, in particular, during peak period. Except for some areas, the simulation results were similar to the actual measured values.

Figure 4. Major analysis points on the satellite image map.

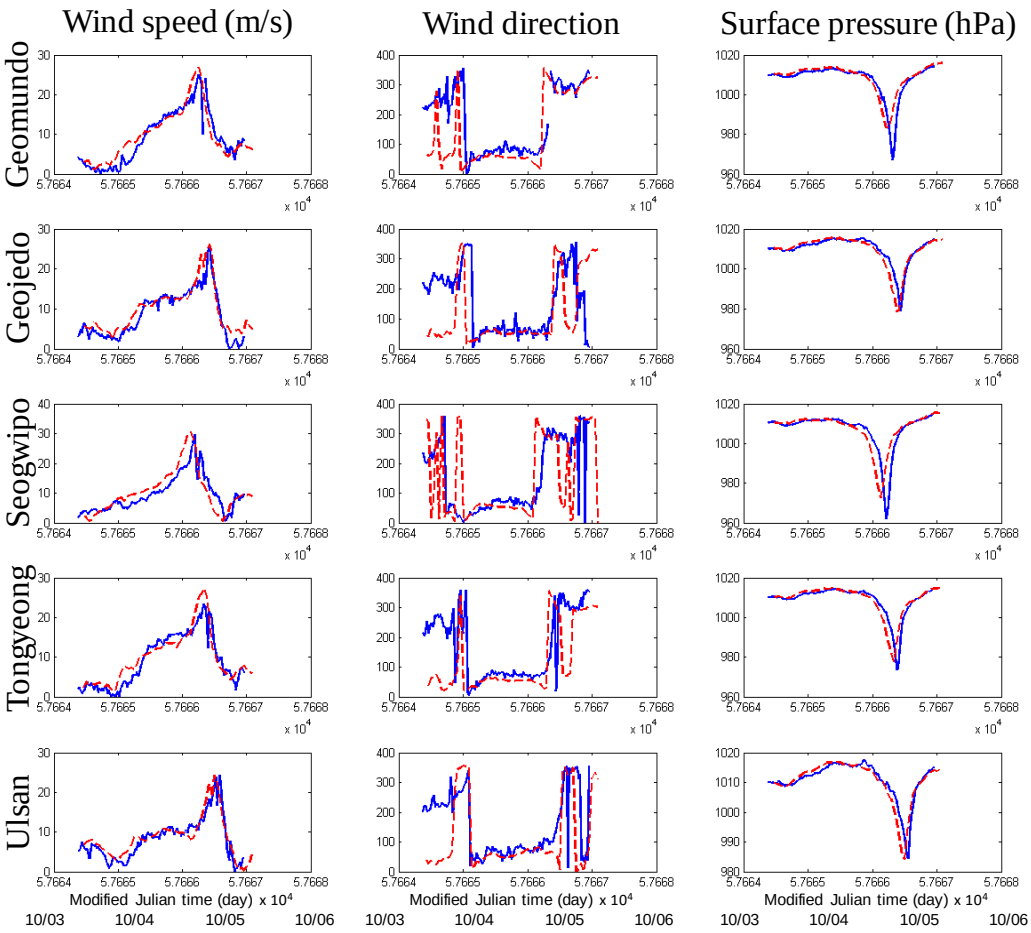

Figure 5. Verification of typhoon modeling by WRF (solid blue lines and dashed red lines denote the observed and simulated results, respectively).

Figure 6 shows that the visualization of the cloud and accumulated precipitation of typhoon CHABA calculated from WRF. VAPOR (Visualization and Analysis Platform for Ocean, Atmosphere, and Solar Researchers) module provides a Python editor that can make new variable. Because there is no variable in WRF output for visualization of the cloud and accumulated precipitation, we tried to make new variable for the cloud and accumulated precipitation using Python editor. To describe the cloud like satellite image, a new variable is created by combining QCLOUD (liquid water mixing ratio) and QICE (ice mixing ratio) of WRF variables, and is visualized using Direct Volume Rendering (DVR) module on high resolution cartographic map, which is generally used for realistic visualization of 3D variables. The distribution of accumulated precipitation, which is obtained from combination of RAINC (cumulus scheme of precipitation) and RAINNC (microphysics scheme of precipitation), is visualized the 2D module at a time. Through this figure, the change of accumulated precipitation could be investigated along moving trajectory of typhoon. To clarify the trajectory of the typhoon cloud, the color map of 60 mm or less was treated transparently in order to consider only the movement characteristics for the extreme rainfalls by the typhoon.

Figure 7 shows that the visualization of storm surge height around South Korea calculated from FVCOM. Because FVCOM is unstructured grid model, VAPOR does not support the direct visualization of FVCOM's results yet. Thus, we have to convert the data from unstructured grid to structured grid using the Inversed Distance Weight (IDW) interpolation within variable effective circle for the treatment of coastal landward boundaries. FVCOM calculates the variation of water level due to the typhoon's property, such as pressure and wind forcing around South Korea Sea.

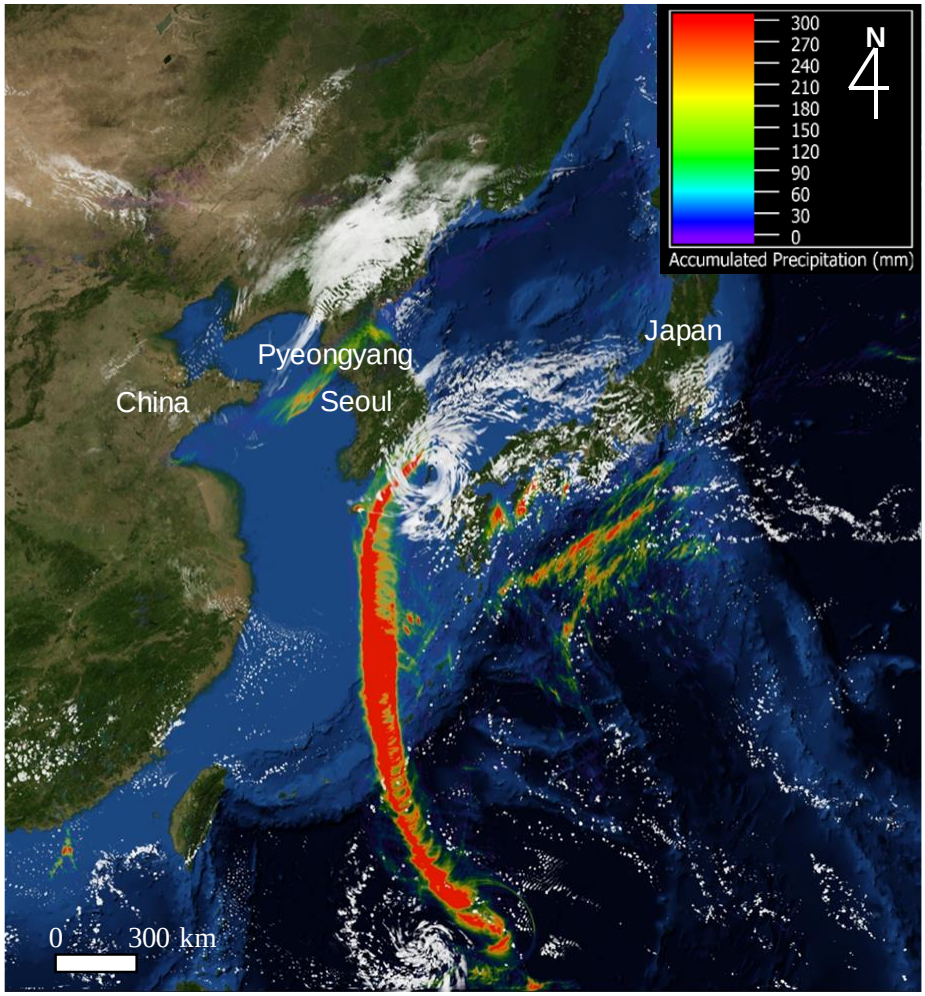

Figure 6. Visualization of cloud and accumulated precipitation of the typhoon.

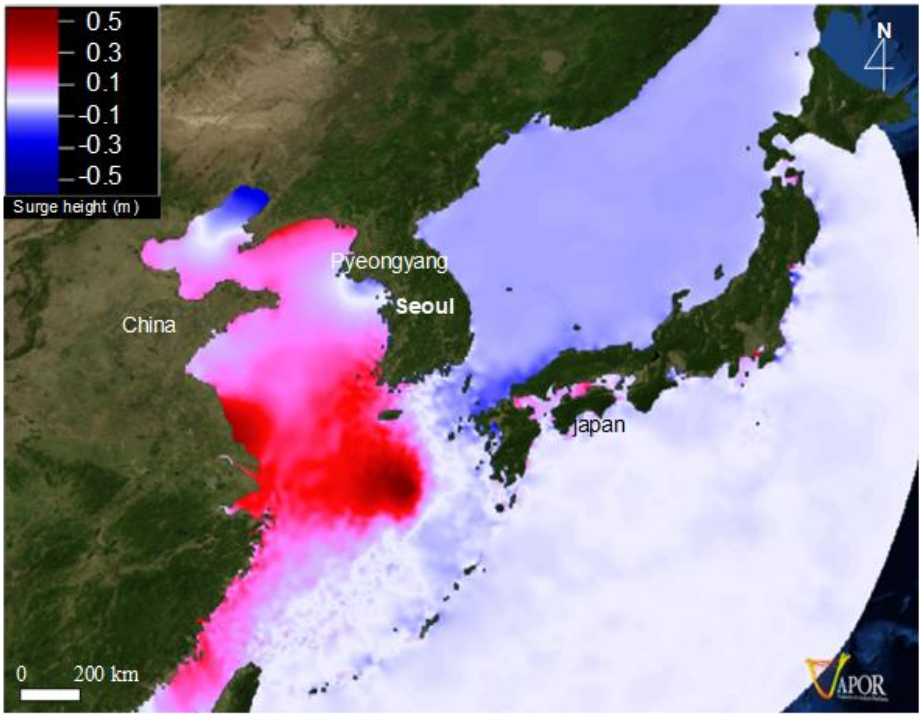

Figure 7. Visualization of storm surge height around South Korea.

Figure 8 shows the comparison of time series of surge height between the simulation and observation. FVCOM underestimated the surge height about 30 cm averagely. An inverse barometer effect is estimated the atmospheric pressure anomaly, and cause the sea level rise about 1 cm per 1 hPa anomaly [33]. In other words, the sea level due to the inverse barometer effect is smaller about 20 cm than real phenomenon. As mentioned above, the underestimation of typhoon-driven air pressure in WRF result in the underestimation of surge during typhoon 'CHABA'. As the typhoon approaches, the surge height is increased due to the strong wind and low pressure, and a negative surge was generated in the Eastern Sea because the water body might be transported to the southern sea of the South Korea due to the counterclockwise movement of the typhoon.

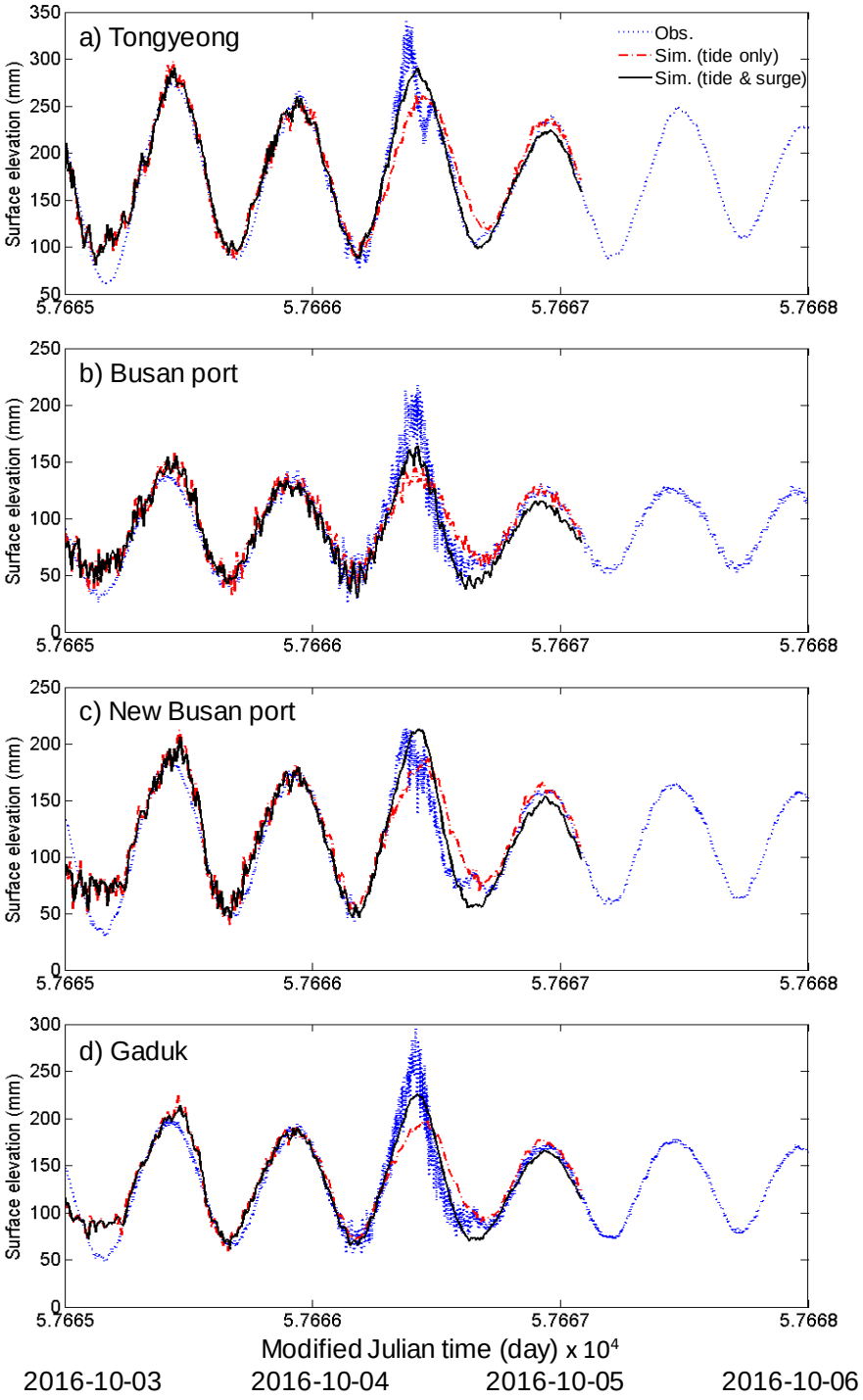

Figure 8. Verification of typhoon-induced surge by using FVCOM: (**a**) Tongyeong; (**b**) Busan port; (**c**) New Busan port; (**d**) Gaduk.

Wave setup increases the mean sea level due to the wave breaking toward shore [29]. But, our surge modeling did not consider wave setup which plays important role in surge, and this additionally affected the underestimation of surge height. Therefore, to consider the wave-driven effect on downscaling for coastal inundation, we simulated the wave motion using SWAN. And simulated wave height is depicted in Figure 9 with contour map. Figure 10 shows the verification of wave modeling. The maximum significant wave height is about 12 m, and the peak period is about 10–15 s when typhoon 'CHABA' approaches near South Korea. The significant wave height is increased by the approaching typhoon southern sea of the South Korea, and it was found that the simulation is not much different from observed data.

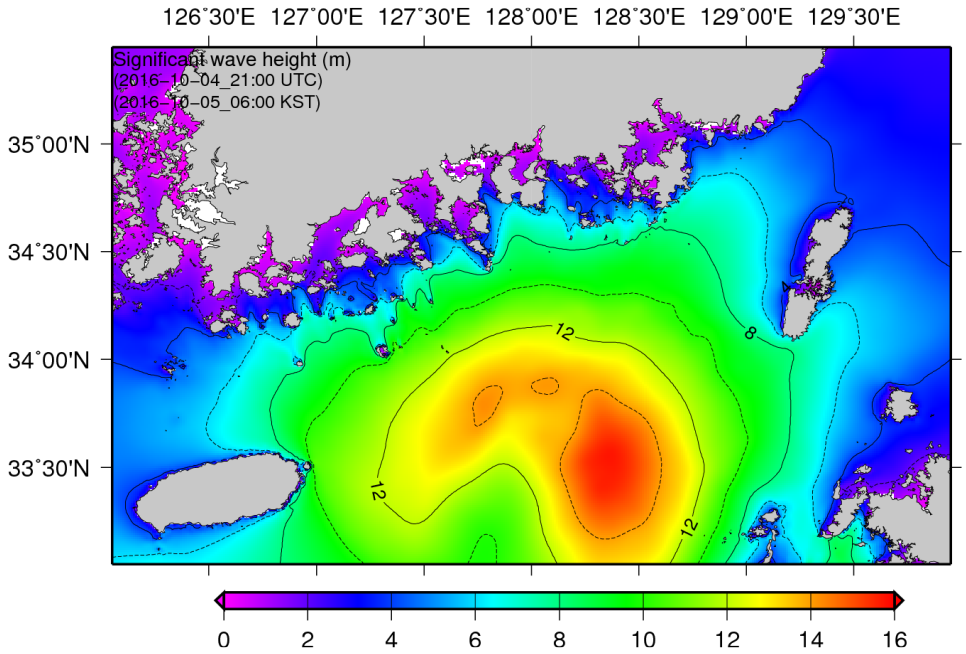

Figure 9. Contour map of simulated significant wave height near the application site.

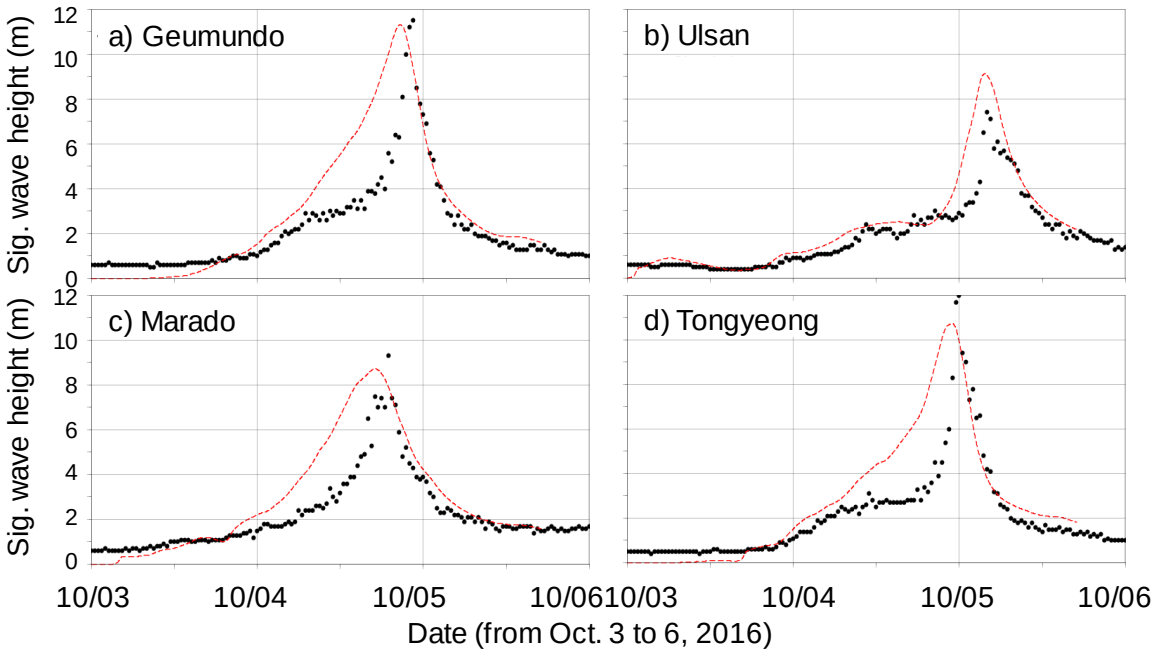

Figure 10. Verification of typhoon-induced wave by SWAN (black scatter: observed results; red dashed line: simulated results).

The Korea Hydrographic and Oceanographic Agency (KHOA) is the national observation agency for the hydrography and oceanography in South Korea and provides the public observation of the oceanic phenomena such as tides, ocean currents, water temperature and salinity. To prove the accuracy of the model application in this research, the validation data were collected from KHOA and compared with the simulated results of case OD1 (Figure 11 and Table 4).

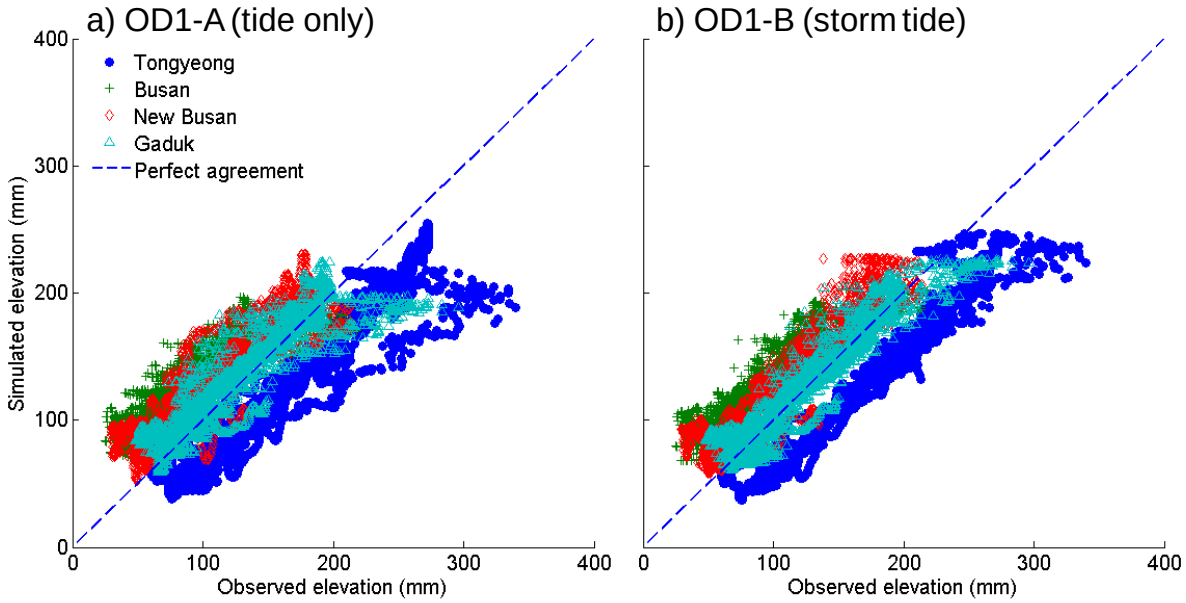

Figure 11. Scatter plot of observed versus simulated values of typhoon-induced wave by SWAN.

Table 4. RMSE results of the model simulation (unit: mm).

Stations	OD1-A (Tide only)	OD1-B (Storm Tide)
Tongyeong	44.20	43.54
Busan port	44.05	38.66
New Busan port	29.06	25.12
Gaduk	20.86	15.25

From the results of comparison, the applied model captures the observed wave elevation well with both cases, OD1-A (tide only) and OD1-B (storm tide case). And differences of the OD1-A case were calculated slightly larger than OD1-B. It is concluded that the consideration of wind speed can improve the model accuracy.

The typhoon-induced coastal inundation in the Busan could result from the strong wave and surge simultaneously. The mean sea level was raised by the typhoon-induced surge, and at same time the typhoon-induced wave with a long period of more than 10 s actually led to the coastal inundation. Finally, Figure 12 shows the simulation result of coastal inundation near Busan combining the surge and wave effect, and the inundation occurred on the southeast coast of Busan, and the inundation height was about 2.5 m near Marine City. In the simulation, considering only surge, a maximum surge height was about 1 m, and the coastal inundation was not estimated. While, by considering the irregular wave height with 1 s interval obtained by JONSWAP spectrum, the flooding near the lower coastal region could be revealed with consideration of surge height and wave height together. Additionally, it is remarkable that the two regions where the inundation height of the simulation results were relatively high are very vulnerable to damage due to the high population density (Haeundae beach and Marine city) and the container dense area (Gamman container terminal). Fortunately, due to the installation of a submerged breakwater to prevent the loss of sand at Haeundae Beach, the beach is not damaged. On the other hand, the Marine city suffered massive property damage and human damage from flood inundation as simulated (Figure 13).

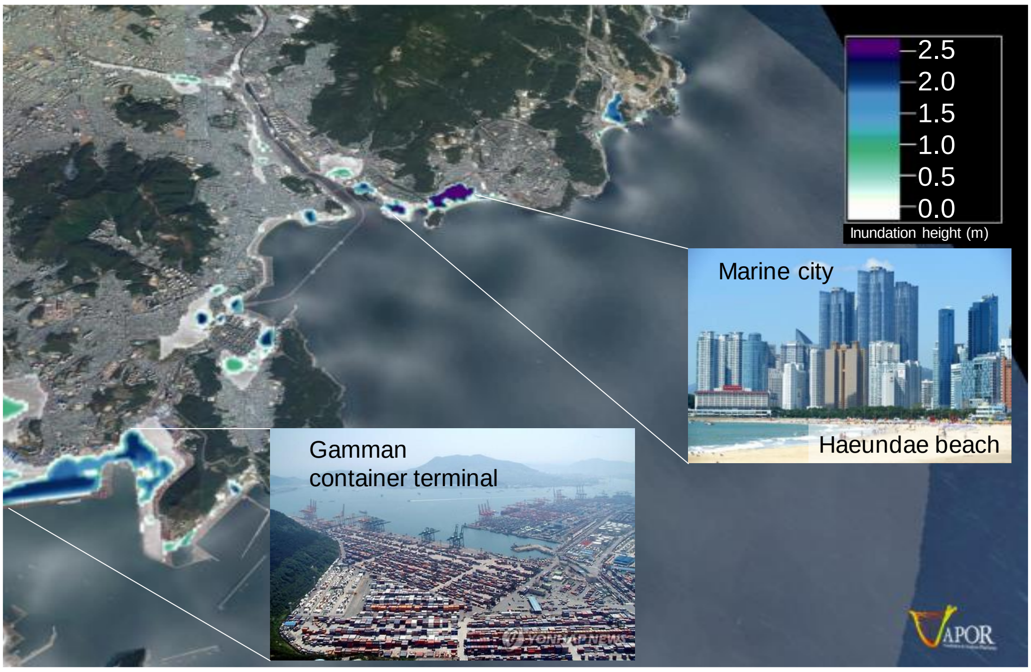

Figure 12. Visualization of coastal inundation results on the South coast near Busan city.

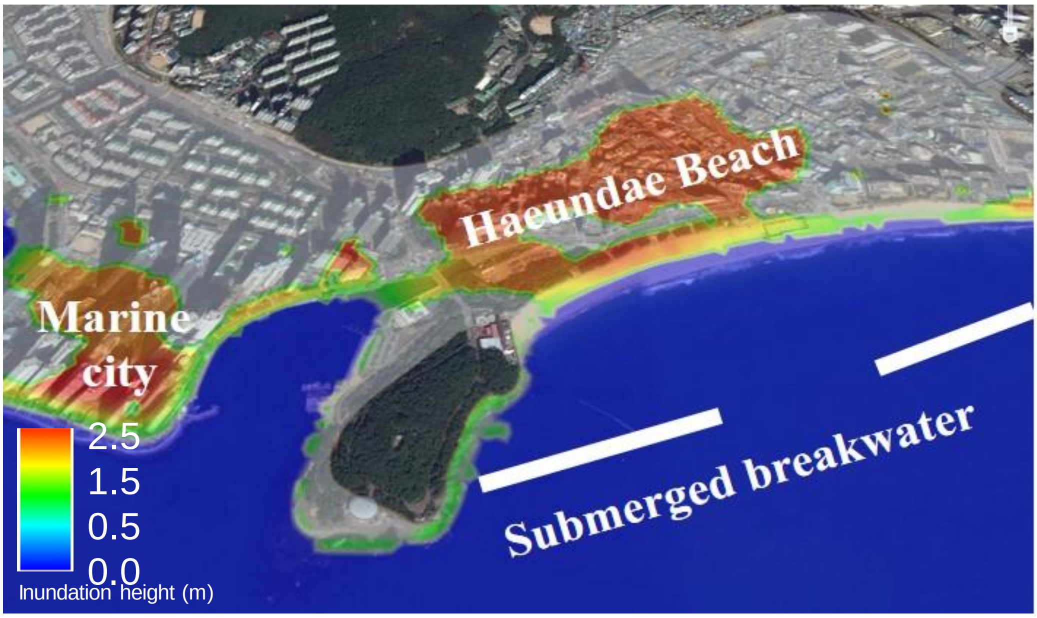

Figure 13. Simulated 2-D contour map with peak coastal inundation.

4. Conclusions and Future Works

In the absence of an integrated system to prevent and respond to various natural disasters at present, it is important to predict and analyze future natural disasters scientifically, accurately, rapidly, and efficiently. Particularly in the case of typhoons, which cause great damage in Korea. The frequency of typhoons in the Western Pacific region is expected to decrease, but their intensity is expected to be greater as climate change accelerates, which is why a more active prevention and response system is needed. Moreover, to respond to disaster immediately and to understand physical phenomena, more accurate prediction system with high resolution is absolutely necessary. The prediction system in K-DMSS (KISTI Decision-Making Support System) is an optimal disaster prediction automation system based on the HPC optimized in South Korea.

In this work, WRF, FVCOM, unSWAN, and downscaled FVCOM were operated for prediction of the Typhoon 'CHABA'-induced inundation, based on the KISIT HPC system. The coastal

inundation could be caused by typhoon-driven surge and wave, and we combined the storm tide height obtained from surge modeling and the irregular wave height which is calculated by JONSWAP spectrum, and applied combined result to the one-way downscaling for coastal inundation to simultaneously consider the effects of surge and wave. From the comparison of the simulation results, model accuracy of the downscaling method has proved. Thus, we have found new possibilities in downscaling methods for coastal inundation.

However, our numerical simulation of coastal inundation is overestimated because of ignoring the effect of submerged breakwater installation. The initial purpose of the submerged breakwater was wave energy dissipator which can reduce the wave-driven inundation in beach and coast. Therefore, the submerged breakwater must be considered in numerical simulation for integrated coastal inundation to analyze flood inundation [28].

In addition, the installation of the submerged structures had significant effect on coastal flooding, that is, the structure dissipates the energy of water motion [3,34–36]. The detail land cover of coastal landward boundaries must be applied to the numerical study for coastal flooding. In addition, 2D numerical simulation tends to underestimate storm surge as compared with 3D simulation, because the stratified condition accounts for much of the water elevation [1,29,37]. Although 3D simulation requires a relatively high computing cost, this is very necessary for the accurate prediction of surge and coastal inundation.

Author Contributions: Conceptualization, D.J. and C.-H.J.; methodology, D.J.; validation, S.P., D.J. and W.K.; formal analysis, C.-H.J.; investigation, W.K.; resources, D.J.; data curation, W.K.; writing—original draft preparation, D.J.; writing—review, editing and visualization, S.P.; supervision, C.-H.J.; project administration, W.J.; funding acquisition, W.J. All authors have read and agreed to the published version of the manuscript.

Funding: This research was supported by Ministry of Science, ICT, Republic of Korea (Project No. K-20-L01-C06-S01).

Conflicts of Interest: The authors declare no conflict of interest.

References

1. Sun, Y.; Chen, C.; Beardsley, R.C.; Xu, Q. Impact of current-wave interaction on storm surge simulation: A case study for Hurricane Bob. *J. Geophys. Res. Ocean.* **2013**, *118*, 2685–2701, doi:10.1002/jgrc.20207.
2. Beardsley, R.C.; Chen, C.; Xu, Q. Coastal flooding in Scituate (MA): A FVCOM study of the 27 December 2010 nor'easter. *J. Geophys. Res. Ocean.* **2013**, *118*, 6030–6045, doi:10.1002/2013JC008862.
3. Yoon, J.J.; Shim, J.S. Estimation of storm surge inundation and hazard mapping for the southern coast of Korea. In Proceedings of the 12th International Coastal Symposium, Plymouth, England, 1 January 2013; ISSN 0749-0208, doi:10.2112/SI65-145.1.
4. Nakamura, R.; Shibayama, T.; Esteban, M. Future typhoon and storm surges under different global warming scenarios: Case study of typhoon Haiyan. *Nat. Hazards* **2016**, *82*, 1645–1681, doi:10.1007/s11069-016-2259-3.
5. Mao, M.; Xia, M. Dynamics of wave–current–surge interactions in Lake Michigan: A model comparison. *Ocean Model.* **2017**, *110*, 1–20, doi:10.1016/j.ocemod.2016.12.007.
6. Wolf, J. Coastal flooding: Impacts of coupled wave-surge-tide models. *Nat. Hazards* **2009**, *49*, 241–260, doi:10.1007/s11069-008-9316-5.
7. Booij, N.; Holthuijsen, L.H.; Ris, R.C. The SWAN wave model for shallow water. *Proceedings of the 25th International Conference on Coastal Engineering*, Orlando, FL, USA, 2–6 September **1996**, 668–676, doi:10.1061/9780784402429.053.
8. Yuk, J.-H.; Park, J.; Joh, M. Modelling of storm-induced seawater flooding in the Suyeong River area, South Korea: A case study due to the storm surge and waves during Typhoon Sanba. *J. Coast. Res.* **2018**, *85*, 746–750, doi:10.2112/SI85-150.1.
9. Ku, H.; Maeng, J.; Lee, H. Estimation of coastal inundation area by typhoon-induced surges. 2018 OCEANS-MTS/IEEE Kobe Techno-Oceans, Kobe, Japan, 28–31 May 2018; p. 8559192, doi:10.1109/OCEANSKOBE.2018.8559192.
10. Climate Change: Global Sea Level. Available online: https://www.climate.gov/news-features/understanding-climate/climate-change-global-sea-level (accessed on 23 March 2020).

11. Song, D.; Guo, L.; Duan, Z.; Xiang, L. Impact of major typhoons in 2016 on sea surface features in the Northwestern Pacific. *Water* **2018**, *10*, 1326, doi:10.3390/w10101326.
12. Wang, Y.H.; Lee, I.H.; Wang, D.P. Typhoon induced extreme coastal surge: A case study at Northeast Taiwan in 1994. *J. Coast. Res.* **2005**, *213*, 548–552, doi:10.2112/03-0026.1.
13. Hallermeier. R. J.; Rhodes, P.E. Generic Treatment of Dune Erosion for 100-Year Event. In Proceedings of the 21st International Conference on Coastal Engineering, Costa del Sol-Malaga, Spain, 20–25 June 1988; ASCE: Costa del Sol-Malaga, Spain, 1988, doi:10.1061/9780872626874.09.
14. Vasseur, B.; Hequette, A. Storm surges and erosion of coastal dunes between 1957 and 1988 near Dunkerque (France), southwestern North Sea. *Geol. Soc.* **2000**, *175*, 99–107, doi:10.1144/GSL.SP.2000.175.01.09.
15. Morton, R.; Factors, A. Controlling storm impacts on coastal barriers and beaches: A preliminary basis for near real-time forecasting. *J. Coast. Res.* **2002**, *18*, 486–501.
16. Gencarelli, R.; Tomasicchio, G.R.; Kobayashi, N.; Johnson, B.D. Beach profile evolution and dune erosion due to the impact of Hurricane Isabel. *Coast. Eng.* **2008**, 1697-1709, doi:10.1142/9789814277426_0141.
17. O'Shea, M.; Murphy, J. Predicting and monitoring the evolution of a coastal barrier dune system postbreaching. *J. Coast. Res.* **2013**, *29*, 38–50, doi:10.2112/JCOASTRES-D-12-00176.1.
18. Hatzikyriakou, A.; Lin, N. Simulating storm surge waves for structural vulnerability estimation and flood hazard mapping. *Nat. Hazards* **2017**, *89*, 939–962, doi:10.1007/s11069-017-3001-5.
19. Schambach, L.; Grilli, A.R.; Grilli, S.T.; Hashemi, M.R.; King, J.W. Assessing the impact of extreme storms on barrier beaches along the Atlantic coastline: Application to the southern Rhode Island coast. *Coast. Eng.* **2018**, *133*, 26–42, doi:10.1016/j.coastaleng.2017.12.004.
20. National Assessment of Hurricane-Induced Coastal Erosion Hazards: Gulf of Mexico. Available online: https://olga.er.usgs.gov/data/NACCH/GOM_erosion_hazards_metadata.html (accessed on 27 February 2020).
21. Pries, A.J. *Hurricane Impacts on Coastal Dunes and Spatial Distribution of Santa Rosa Beach Mice (Peromyscus Polionotus Leucocephalus) in Dune Habitats*; Master's Thesis, University of Florida, Gainesville, FL, USA, May 2006.
22. Gaeta, M.G.; Bonaldo, D.; Samaras, A.G.; Carniel, S.; Archetti, R. Coupled wave-2D hydrodynamics modeling at the Reno river mouth (Italy) under climate change scenarios. *Water* **2018**, *10*, 1380, doi:10.3390/w10101380.
23. Postacchini, M.; Lalli, F.; Memmola, F.; Bruschi, A.; Bellafiore, D.; Lisi, I.; Zitti, G.; Brocchini, M. A model chain approach for coastal inundation: Application to the bay of Alghero. *Estuar. Coast. Shelf Sci.* **2019**, *219*, 56–70, doi:10.1016/j.ecss.2019.01.013.
24. Aoki, K.; Isobe, A. Application of finite volume coastal ocean model to hindcasting the wind-induced sea-level variation in Fukuoka bay. *J. Oceanogr.* **2007**, *63*, 333–339, doi:10.1007/s10872-007-0032-7.
25. Chen, C.; Qi, J.; Li, C.; Beardsley, R.C.; Lin, H.; Walker, R.; Gates, K. Complexity of the flooding/drying process in an estuarine tidal creek salt-marsh system: An application of FVCOM. *J. Geophys. Res.* **2008**, *113*, C07052, doi:10.1029/2007JC004328.
26. Weisberg, R.H.; Zheng, L. Hurricane storm surge simulations comparing three-dimensional with two-dimensional formulations based on an Ivan-like storm over the Tampa Bay, Florida region. *J. Geophys. Res.* **2008**, *113*, C12001, doi:10.1029/2008JC005115.
27. Westerink, J.J.; Luettich, R.A.; Feyen, J.C.; Atkinson, J.H.; Dawson, C.; Roberts, H.J.; Powell, M.D.; Dunion, J.P.; Kubatko, E.J.; Pourtaheri, H. A basin-to channel-scale unstructured grid hurricane storm surge model applied to Southern Louisiana. *Mon. Weather Rev.* **2008**, *136*, 833–864, doi:10.1175/2007MWR1946.1.
28. Qi, J.; Chen, C.; Beardsley, R.C.; Perrie, W.; Cowles, G.W.; Lai, Z. An unstructured-grid finite-volume surface wave model (FVCOM-SWAVE): Implementation, validations and applications. *Ocean Model.* **2009**, *28*, 153–166, doi:10.1016/j.ocemod.2009.01.007.
29. Dukhovskoy, D.S.; Morey, S.L. Simulation of the hurricane dennis storm surge and considerations for vertical resolution. *Nat. Hazards* **2011**, *58*, 511–540, doi:10.1007/s11069-010-9684-5.
30. Feng, X.; Yin, B.; Yang, D. Development of an unstructured-grid wave-current coupled model and its application. *Ocean Model.* **2016**, *104*, 213–225, doi:10.1016/j.ocemod.2016.06.007.
31. Qi, J.; Chen, C.; Beardsley, R.C. FVCOM one-way and two-way nesting using ESMF: Development and validation. *Ocean Model.* **2018**, *124*, 94–110, doi:10.1016/j.ocemod.2018.02.007.

32. Hasselmann, K.; Barnett, T.P.; Bouws, E.; Carlson, H.; Cartwright, D.E.; Enke, K.; Ewing, J.A.; Gienapp, H.; Hasselmann, D.E.; Kruseman, P.; et al. *Measurements of Wind-wave Growth and Swell Decay During the Joint North Sea Wave Project (JONSWAP)*; Deutches Hydrographisches Institute: Hamburg, Germany, **1973**; A(8), Nr. 12. Available online: http://resolver.tudelft.nl/uuid:f204e188-13b9-49d8-a6dc-4fb7c20562fc (accessed on 20th March 2020).
33. Gill, A.E. *Atmosphere-ocean Dynamics*; Academic Press Inc.: New York, NY, USA, 1982; Volume 30.
34. Zidan, A.R.; Rageh, O.S.; Sarhan, T.E.; Esmail, M. Effect of breakwaters on wave energy dissipation (Case study: Ras El-bar Beach, Egypt). *Int. Water Technol. J.* **2012**, *2*, 268–283.
35. Ferreira, C.M.; Irish, J.L.; Olivera, F. Uncertainty in Hurricane Surge Simulation due to Land Cover Specification. *J. Geophys. Res. Ocean.* **2014**, *119*, 1812–1827, doi:10.1002/2013JC009604.
36. Wamsley, T.; Cialone, M.; Smith, J.M.; Ebersole, B.A.; Grzegorzewski, A.S. The potential of wetlands in reducing storm surge. *Ocean Eng.* **2010**, *37*, 59–68, doi:10.1016/j.oceaneng.2009.07.018.
37. Kodaira, T.; Thompson, K.R.; Bernier, N.B. The Effect of Density Stratification on the Prediction of Global Storm Surge. *Ocean Dyn.* **2016**, *66*, 1733–1743, doi:10.1007/s10236-016-1003-6.